On the Fatigue Crack Growth Analysis of Spliced Plates under Sequential Tensile and Shear Loads

Xiaobo Yu

Air Vehicles Division, Defence Science and Technology Organisation,
506 Lorimer Street, Fishermans Bend, VIC 3207, Australia
Fax: +61-(0)3-9626-7089, E-mail: xiaobo.yu@dsto.defence.gov.au

ABSTRACT. The spliced plates on an aircraft with wing mounted power plant are subject to sequentially applied tensile and shear load cycles, with far more tensile cycles than shear cycles. This paper aims to propose an approach to address the fatigue crack growth under this scenario. Current understanding on fatigue crack growth behaviours was reviewed, focusing on crack surface interferences and fatigue crack growth mechanisms under non-proportional mixed-mode loads. A generic spliced plate was analysed using non-linear finite element modelling. The analysis revealed shear-induced-bearing at fastener holes, and predicted both shear-induced- K_I and shear-induced- K_{II} at a 0° crack emanating from the fastener hole edge. When the crack is short relative to the fastener hole radius, the shear-induced- K_I is dominant therefore it has the potential to cause shear-induced mode I overload. As the crack grows longer, the shear-induce- K_{II} increases, and depending on the load level, this may lead to both short-range acceleration and long-range retardation. Through the above analysis, the engineering problem of fatigue crack growth in a spliced plate under sequential tensile and shear loads was converted into a more generally understood problem of fatigue crack growth under cyclic mode I plus intermittent cyclic mixed-mode loads.

INTRODUCTION

Aircraft structures are subject to spectrum loading from multiple sources. Yet in aircraft structural integrity management, the fatigue crack growth (FCG) is usually predicted assuming a uniaxial load spectrum. This is appropriate in most cases where the multi-axial loads at the global level are transformed by load path constraints into an approximately uniaxial load spectrum at the local fatigue critical area. However, not all the global multi-axial loads can be reduced to a local uniaxial spectrum. For instance, on an aircraft with wing mounted power plant, some areas of its wing skin panels, including the spliced joint as schematically illustrated in Fig. 1, may experience both tensile and shear load spectrums. The tensile load is caused by the span-wise bending of the wing box, which mainly exists when the aircraft is in air. Meanwhile, the shear load is caused by the wing box torsion due to engine inertia, which is predominant during the landing and dynamic taxiing phases. Notably, the variation of the tensile and shear loads

occur almost sequentially, and there are far more tensile cycles than shear cycles. This may be viewed as a special case of non-proportional loading,

For the spliced plate depicted in Fig. 1, a fatigue crack usually starts from the edge of a fastener hole. Under the sequential tensile and shear loads, the FCG behaviour is affected by a number of extra factors, in addition to those that apply to a unixial FCG. These extra factors include: (i) load tranferring through fastener holes under nominal tensile and shear loads, (ii) changes of effective fatigue driving force due to mixed-mode crack surface interference, and (iii) potential alternation of FCG mechanisms under non-proportional tensile and shear loads.

At present, the understanding of the above three extra factors is still limited, and no reliable FCG prediciton tool is readily available. In the area of multi-axial fatigue analysis, most of the advances are at the forefront of fatigue life predictions as reviewed in [1]. Only a few investigations [2-7] focused on the FCG under non-proportional tensile and shear loads, and none of these has considered the load-bearing effects of a fastener hole under nominal shear loads.

The purpose of this paper is therefore to propose an approach to address the FCG in a spliced plate under sequential tensile and shear loads. This will be based on a review of the general understanding of FCG under non-proportional mixed-mode loads, and a detailed stress analysis of a generic spliced plate under tension and shear.
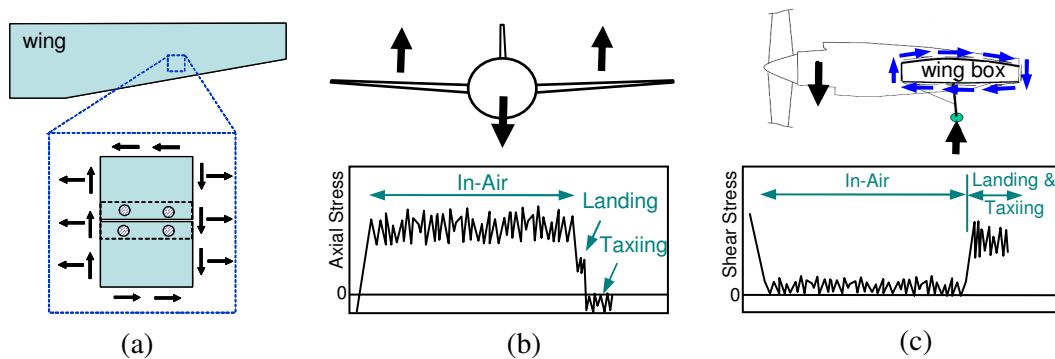

Figure 1. (a) A splice joint subject to tensile and shear loads; (b) Tensile load resulted from wing box span-wise bending; and (c) Shear load resulted from wing box torsion.

GENERAL UNDERSTANDING OF FCG UNDER MIXED-MODE LOADS

Local Fatigue Driving Forces under Nominal Loads

In FCG analysis based on linear elastic fracture mechanics, the local fatigue driving forces are characterised by stress intensity factors, noted as K_I, K_{II} and K_{III}, respectively corresponding to the mode I (opening), mode II (in-plane shear) and mode III (out-of-plane shear) deformations near a crack tip. This paper is concerned with the K_I and K_{II} mixed-mode only.

In general, the modes of local FCG driving force depend on the load direction in relation to the crack orientation and can be further altered by local features near the crack tip. On an aircraft structure, fatigue cracks usually emanate from the edge of an open or fastener hole. In the case of an open hole, the K_{II}-value approaches zero when the crack is short relative to the hole dimension. In the case of a fastener hole, the relationships between K_I and tensile force – both of by-pass and bearing natures – are known facts and have been incorporated into FCG prediction tools. Nevertheless, the K_I and K_{II} relationships to the nominal shear load are yet to be established. This relationship will be investigated in this study.

Effective Mixed Mode I and II Stress Intensity Factors

For FCG under cyclic mode I loads, the effective range of K_I is known to be affected by crack closure, which arises when the crack surfaces are wedged opened by one of the five mechanisms [8] including: plastic wake, oxidation build-ups, roughness asperity, trapped fluids and phase-transformations. Meanwhile, under cyclic mode II loads, shear attenuation [9] was noticed, which may explain why the K_{II} effective range is much less than the applied one.

Nevertheless, a simple addition of mode I crack closure and mode II attenuation does not give a full description of the crack surface interference (CSI) under mixed-mode loads. Both modelling [10, 11] and experimental studies [12, 13] indicate that the K_I and K_{II} variations can be coupled due to cyclic sliding along facets of crack surface asperities, as schematically illustrated in Fig. 2.

The measurement of effective K_I and K_{II} ranges under mixed-mode loads is more complicated than the crack closure measurement under a pure mode I load. The main difficulty arises when the effective K_I and K_{II} variations need to be determined for a "closed" crack that accommodates sliding along the asperity facets. A reliable and convenient approach is yet to be developed for this purpose.
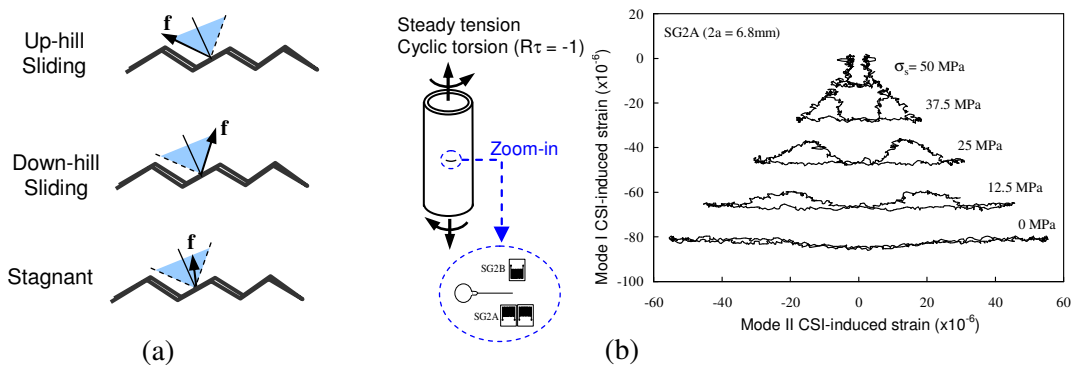

Figure 2. (a) Forces at asperity facets during varied stages of crack surface interference ; (b) Experimental evidence of CSI-induced K_I variation [12]

FCG Mechanisms and Path

Under the mixed-mode loading conditions, most of the published fatigue test results indicated that a fatigue crack deviates to a direction that features a tensile-mode FCG mechanism. This direction can be approximately predicted by the maximum tangential stress (MTS) criterion [14]. For a Paris-region FCG, fatigue striations are usually observed on fracture surfaces.

Shear-mode FCG was observed in limited scenarios, and is subject to a number of conditions including material, load, constraint and crack tip acuity. In general, a shear-mode FCG is easier to develop in aluminium alloys than in steels [15], and easier to develop from a sharp crack tip than from a notch edge [16]. The shear-mode FCG can also be promoted by applying a compressive load to suppress mode I branching [17], or applying a non-proportional cyclic mode I and cyclic mode II loads [2-7]. In addition, a short distance of shear-mode growth was also reported [18] before mode I branching.

Fig, 3 compares the FCG from a mode I pre-crack tip under two types of mixed-mode loads. Under the proportional mixed-mode loads, the FCG path deviates into a direction that can be approximately predicted by the MTS criterion, and striations are observed at the fracture surface. The post-deviation FCG is therefore deemed as mode I growth. Under the non-proportional mixed-mode loads, the FCG deviates to a direction that is about 60° off the MTS prediction. For this particular case, the deviation angle is approximately as predicted by the maximum shear stress (MSS) criterion [19]. The crack surface is featured with dimples instead of striations. The post-deviation FCG is therefore deemed as shear-mode growth. The shear-mode FCG is stable and, under the same applied tensile and shear load ranges, is about 6 times as fast as the mode I FCG.

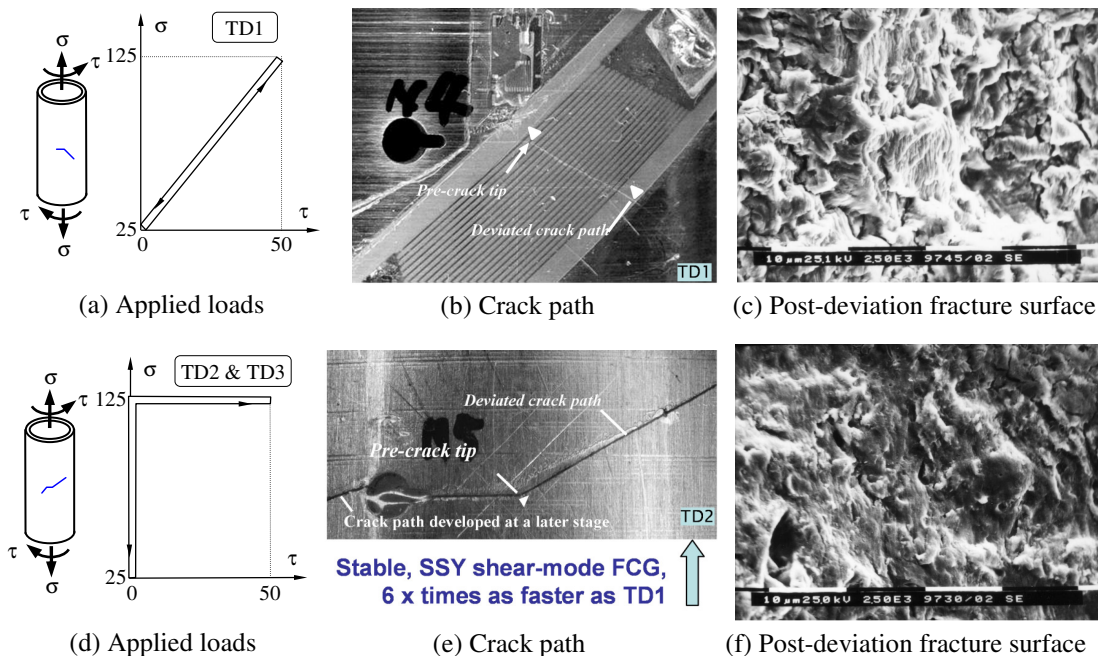| (a) Applied loads	(b) Crack path	(c) Post-deviation fracture surface
(d) Applied loads	(e) Crack path	(f) Post-deviation fracture surface

Figure 3. FCG from a mode I pre-crack, under proportional (a-c), and non-proportional (d-f), mixed-mode loads [12]. (SSY refers to small scale yielding)

NON-LINEAR STRESS ANALYSIS OF A GENERIC SPLICED PLATE

Finite Element Model Definitions

A generic spliced plate is analysed. As depicted in Fig. 4, it consists of two large plates A and B, and a small plate C. The connections between plates A-C and B-C are each through a row of eight fasteners.

The spliced plate was analysed as a planar model using StressCheck v9.2 [20], with two geometrical configurations: (i) without a crack, for which the mesh and boundary conditions are as shown in Fig. 5(a); and (ii) with a $\theta = 0°$ crack emanating from the "R2" fastener hole, for which the mesh near the crack is shown in Fig. 6(a). For each configuration, two load cases were analysed: (i) by-pass tension, $\sigma = 68.9$ MPa, and (ii) shear, $\tau = 68.9$ MPa. The plate-to-fastener contacts were modelled using fastener elements in the StressCheck. The 0° crack path was selected taking into account that the spliced joint on the aircraft was subject to far more tensile cycles than shear cycles.

Planar model:
H = 203.2 mm (8 inch), L = H/4
W = 203.2 mm (8 inch)
WJ = 25.4 mm (1 inch)
TH = 3.175 mm (0.125 inch)
D = 7.938 mm (0.3125 inch)

Materials:
[plane stress, linear elastic]:
Plates: AA, E = 75.2 GPa, μ = 0.397
Fasteners: Steel, E = 200 GPa, μ =0.295
Fastener connection: Rigid
Fastener interference: nil friction,
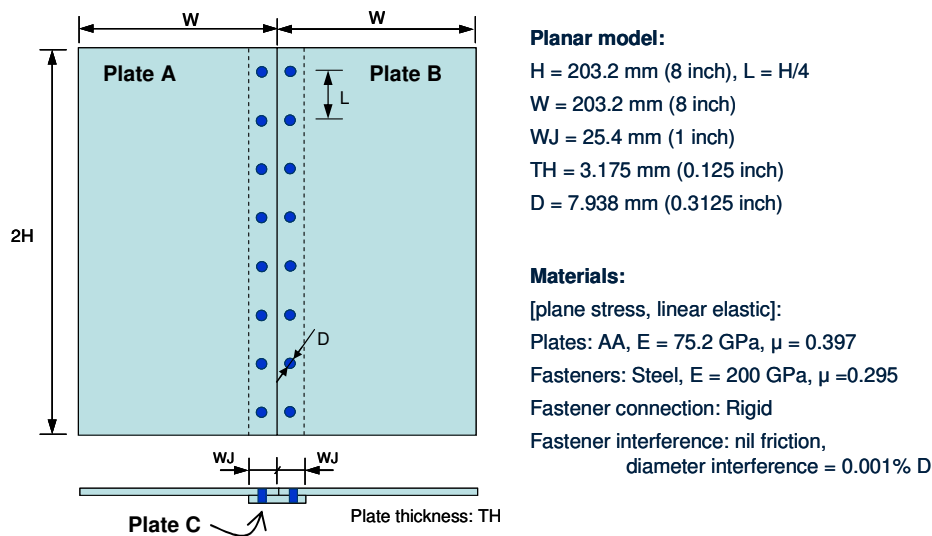   diameter interference = 0.001% D

Figure 4. Cinfiguration of a generic spliced plate.

Results and Discussions

Fig. 5 illustrates the stress distribution in the spliced plate under nominal shear loading. One significant observation is the existence of bearing stress at the fastener holes. Also, the tensile hoop stress maximises at a near $\theta = 0°$ position. These results are different from the stress distributions at an open hole under the same shear loading. For an open hole, the bearing stress does not exist and the maximum hoop stress occurs at the $\theta = -45°$ and $+135°$ positions. As shown in Fig. 6(b), the bearing stress leads to a significant K_I for a small crack. In fact, when a/R < 1 and with the current D/L (=0.3125/2) and σ/τ (=1) ratios, the τ–induced K_I is larger than the σ–induced K_I.

As shown in Fig. 7, the shear-induced-bearing is different from the tension-induced-bearing. Thus the latter should not be directly used to estimate the shear-induced K_I.
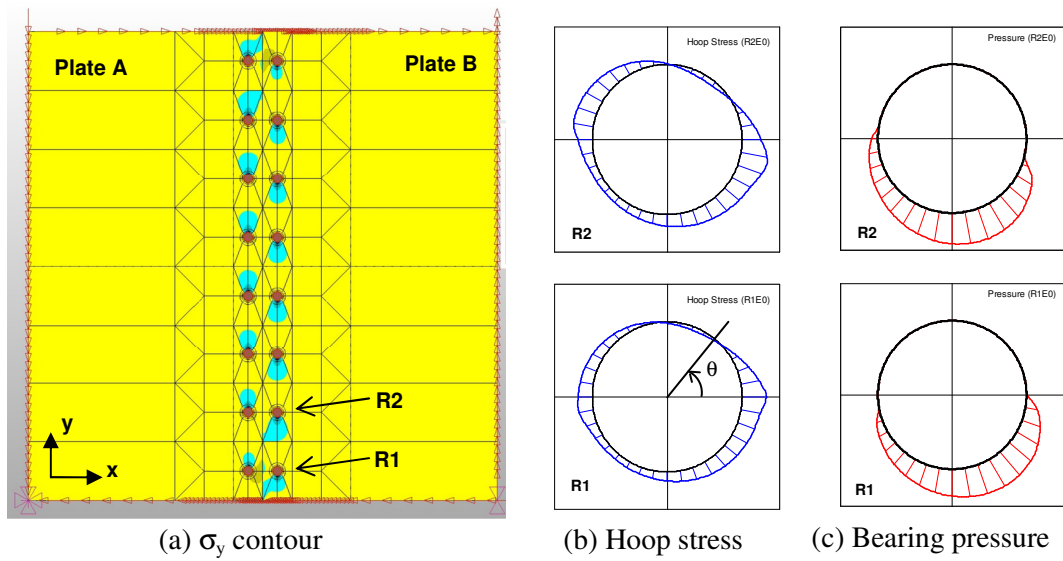
(a) σ_y contour   (b) Hoop stress   (c) Bearing pressure

Figure 5. Stresses in the spliced plate under the nominal shear load.

(a)   (b)
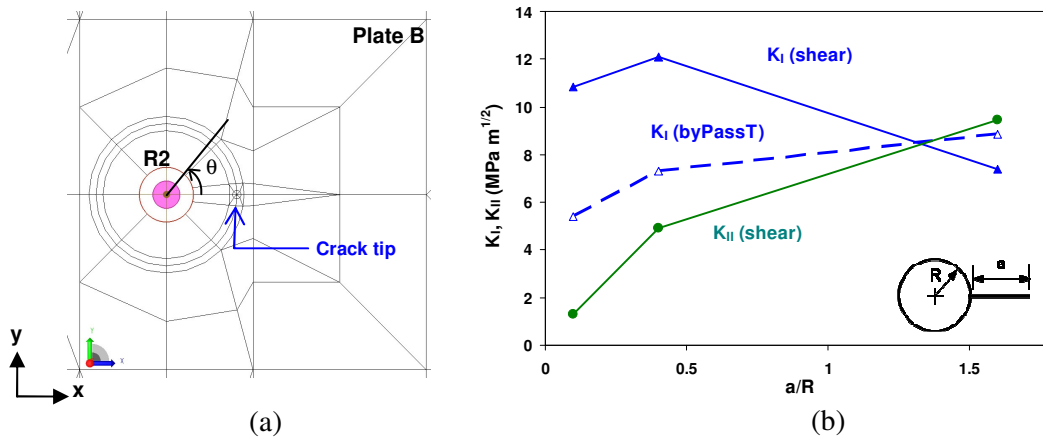
Figure 6. (a) StressCheck mesh near the crack (a/R = 1.6);
(b) Mode I and mode II stress intensity factors under shear and by-pass tension.

$2 \times K_{I\_shear-induced-bearing} = K_{I\_fb}$ $2 \times K_{I\_tension-induced-bearing} = K_{I\_fb} + K_{I\_\sigma}$
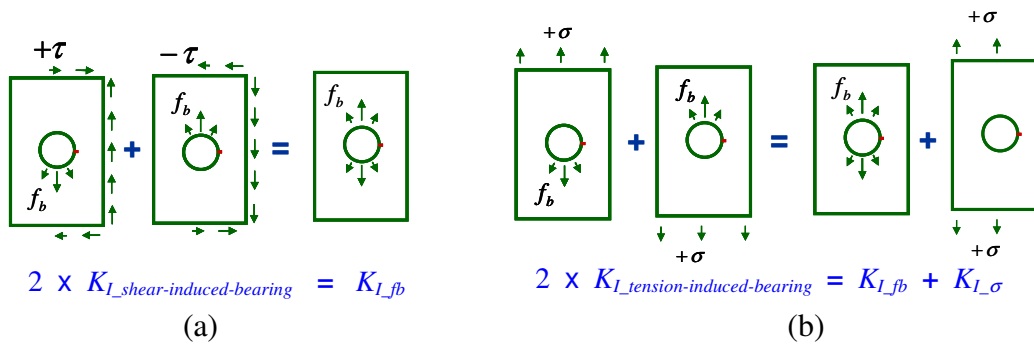
(a)   (b)

Figure 7. K_I estimations for: (a) Shear-induced-bearing; (b) Tension-induced-bearing.

PROPOSAL ON FCG ANALYSIS

In mimicking the spectrum loading on the wing panel joints of a powered aircraft, the current study assumes sequential tensile and shear load cycles on a spliced plate. The number of tensile cycles far exceeds the number of shear cycles. As such, the FCG can be assumed to be dominated by mode I growth under the tensile cycles, and the crack path – as analysed in the previous section – can be assumed as a $0°$ crack emanating from the fastener hole edge. The remain challenging is to estimate the effects of the intermittent shear cycles.

As revealed in the previous section, the nominal shear load applied on a spliced plate can induce both K_I and K_{II} to a $0°$ crack emanating from the fastener hole edge. There are two scenarios here: (i) When the crack is short, the K_I component is dominant, therefore the potential of shear-induced-mode-I overload needs to be assessed; and (ii) As crack grows, the K_{II} component increases and K_I drops after an initial increment, therefore the effects of intermittent mixed-mode loads need to be assessed. In relating to the second scenario, Ref. [21] proposed two competing mechanisms – a short-range mode II induced acceleration and a long-range mode II induced crack closure – to explain FCG under mode I cycles with periodic mode II loading. Here, the short-range acceleration can be related to the shear-mode FCG under non-proportional mixed-mode loads, and the long-range crack closure can be related to the crack surface interference under residual shear deformations. As reported, the long-range mechanism is only effective when applied mode II load is sufficiently large. It is likely that the effective mechanism of the intermittent shear cycles varies as the crack grows.

Through the above analysis, the engineering problem of FCG in a spliced plate under sequential tensile and shear loads is converted into a more generally understood, though still rarely investigated, problem of FCG under cyclic mode I with intermittent cyclic mixed-mode loads. In light of this, further investigations that may be needed to support the airframe structural integrity management are outlined as follows. In respect to the spliced plate, the effects of fastener interference and 3-D corner cracks need to be further investigated, with the consideration of real geometry and dimensions. In respect to the scientific research of FCG under non-proportional mixed-mode loads, more investigations are needed on the crack surface interference, especially on the interaction between mode II deformation and mode I crack closure, and on the intrinsic FCG mechanism under non-proportional cyclic loading.

CONCLUSIONS

A review on FCG under non-proportional mixed-mode load indicates that:
- Variations of K_I and K_{II} are coupled through the sliding along asperity facets;
- A shear-mode FCG can be promoted by non-proportional mixed-mode loads;
- The shear-mode FCG is much faster than a corresponding mode I FCG.

The detailed analysis of a generic spliced plate revealed that, under nominal shear loading:

- Both K_I and K_{II} can be induced at a 0° crack emanating from the fastener hole;
- When the crack is short, the shear-induced-K_I is dominant therefore it has potential to cause shear-induced mode I overload;
- As the crack grows longer, the shear-induce-K_{II} increases therefore it may lead to competing of short-range acceleration and long-range retardation;
- The effects of shear-induced-bearing cannot be approximately represented by an open hole or tension-induced-bearing.

Through the above analysis, the engineering problem of FCG in a spliced plate with sequential tensile and shear loads was converted into a more generally understood problem of FCG with cyclic mode I plus intermittent cyclic mixed-mode loads. Further investigation is suggested.

REFERENCES

1. Fatemi, A. and Shamsaei N. (2011) *Int. J. Fatigue* **33**, 948-958.
2. Nayeb-Hashemi, H. and Taslim, M.E. (1987) *Eng. Fract. Mech.* **26**, 789-807.
3. Wong, S.L., Bold, P.E., Brown, M.W. and Allen, R.J. (1996) *Wear* **191,** 45-53.
4. Yu, X. (1999). PhD Thesis, the University of Sydney, Australia.
5. Doquet, V. and Pommier, S. (2004) *Fatigue Fract. Eng. Mater. Struct.* **27**, 1051-60.
6. Highsmith, S. Jr. (2009) PhD Thesis, Georgia Institute of Technology, USA.
7. Doquet, V., Abbadi, M., Bui, Q. and Pons, A. (2009) *Int. J. Fract.* **159**, 219-232.
8. Suresh, S. and Ritchie R.O. (1984) In: *Fatigue Crack Growth Threshold Concepts*, pp. 227-261, Davidson, D.L. and Suresh, S. (Ed.). TMS-AIME.
9. Smith, M.C. and Smith R.A. (1988) In: *Basic Questions in Fatigue: Volume I., ASTM STP 924*, pp. 260-280, Fong J.T. and Fields R.J. (Ed.)
10. Tong, J., Yates J.R. and Brown M.W. (1995) *Eng. Fract. Mech.* **52**, 613-23.
11. Yu, X. and Abel, A. (1999) *Fatigue Fract. Eng. Mater. Struct.* **22**, 205-13.
12. Yu, X. and Abel, A. (2000) *Fatigue Fract. Eng. Mater. Struct.* **23**, 151-8.
13. Bertolino, G. and Doquet V. (2009) *Eng. Fract. Mech.* **76**, 1574-88.
14. Erdogan, F. and Sih G.C. (1963) *J. Basic Eng.* **85**, 519-27.
15. Otsuka, A., Mori, K., Ohshima, T. and Tsuyama, S. (1981) In: *Advances in Fracture Research, Fracture 81, ICF5*, pp. 1851-8, Francois D. (Ed.)
16. Otsuka, A., Mori, K. and Tohgo K. (1987) In: *Current Research on Fatigue Cracks*, pp. 149-180, Tanaka, T., Jono, M. and Komai K. (Ed.), Elsevier Applied Science.
17. Otsuka, A. and Aoyama M. (1993) In: *Mixed-Mode Fatigue and Fracture, ESIS 14*, pp. 49-60, Rossmanith, H.P. and Miller K.J. (Ed.), Mech. Eng. Publications.
18. Smith, M.C. (1984). PhD Thesis, University of Cambridge, U.K.
19. Otsuka, A., Mori K., and Miyata T. (1975) *Eng. Fract. Mech.* **7**, 429-39.
20. ESRD Inc. (2011) *StressCheck Master Guide, Release 9.2.*
21. Dahlin, P. and Olsson, M. (2008) *Inter. J. Fatigue* 30, 931-41.